ウェブサイト公開用

（様式 10）
（海外特別研究員事業）
令和元年 8 月 1 日

海外特別研究員最終報告書

独立行政法人 日本学術振興会 理事長　殿

採用年度　平成 30 年
受付番号　201860232
氏　　名　山室和彦

（氏名は必ず自署すること）

海外特別研究員としての派遣期間を終了しましたので、下記のとおり報告いたします。
なお、下記及び別紙記載の内容については相違ありません。

記

1. 用務地（派遣先国名）用務地：　マウントサイナイ医科大学　（　アメリカ　国）

2. 研究課題名（和文）社会行動における神経回路基盤の解明とその克服

3. 派遣期間：平成 31 年 1 月 1 日～令和元年 6 月 23 日（174 日間）

4. 受入機関名及び部局名
マウントサイナイ医科大学　精神科

5. 所期の目的の遂行状況及び成果…書式任意　**書式任意（A4 判相当 3 ページ以上、英語で記入も可）**
（研究・調査実施状況及びその成果の発表・関係学会への参加状況等）
（注）「6. 研究発表」以降については様式 10－別紙 1～4 に記入の上、併せて提出すること。

Prefrontal circuitry in control of limbic thalamus requires juvenile social experience to establish adult sociability

Kazuhiko Yamamuro[1-5], Hirofumi Morishita[1-5,#]

[1]Department of Psychiatry, [2]Department of Neuroscience, [3]Department of Ophthalmology, [4]Mindich Child Health and Development Institute, [5]Friedman Brain Institute, Icahn School of Medicine at Mount Sinai, One Gustave L. Levy Place, New York, NY 10029 USA
Corresponding author

Summary

Loneliness is now recognized as an epidemic in the society, impacting mental health. Social isolation during the juvenile critical window is particularly detrimental to the maturation of medial prefrontal cortex (mPFC) and establishment of appropriate levels of adult sociability[1,2] (data not shown). However, the neural circuit mechanisms underlying these phenomena are poorly understood. Here we identify a novel pair of specific mPFC excitatory and inhibitory circuits in control of mouse social behavior whose maturation is profoundly affected by juvenile social experience. We found that transient juvenile social isolation (p21-p35: jSI) leads to a failure to activate adult mPFC neurons projecting to the posterior paraventricular nucleus of thalamus (pPVT), also known as the limbic thalamus, which relays signals to various components of the classical reward circuitry[3], in response to a social encounter (Fig.1). Chemogenetic or optogenetic suppression of this circuit is sufficient to induce social behavior deficits without affecting preference to another natural reward such as food, motor activity or anxiety-related behaviors (Fig.2), while optogenetic stimulation biases sociability (data not shown). Mechanistically, jSI leads to reduced intrinsic excitability of mPFC->pPVT projection neurons and an aberrantly increased inhibitory drive from a subclass of deep layer somatostatin (SST) expressing low-threshold spike (LTS) interneurons[4] (Fig.3), aberrant chemogenetic activation of which reduces sociability (data not shown). Sociability deficits caused by juvenile social isolation are rescued by chemogenetic or optogenetic activation of mPFC->pPVT projection neurons (data not shown). Our results demonstrate mPFC->pPVT projection neurons and associated mPFC LTS-SST interneurons as a novel pair of mPFC circuits which require juvenile social interaction to establish normal circuit function necessary for adult sociability. As these circuits are sensitive to experience-dependent modulation, they are attractive circuit targets for the amelioration of social processing deficits shared across of range of disorders[5]. Ultimately, our study may inspire interventions that improve social processing in neurodevelopmental and psychiatric disorders by specifically targeting prefrontal top-down circuits with techniques such as transcranial magnetic stimulation and/or transcranial direct current stimulation, which can impact sub-cortical hubs, such as PVT.

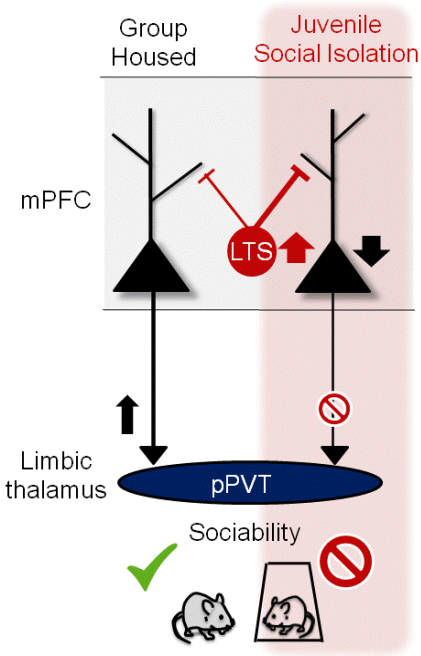

Main Figures

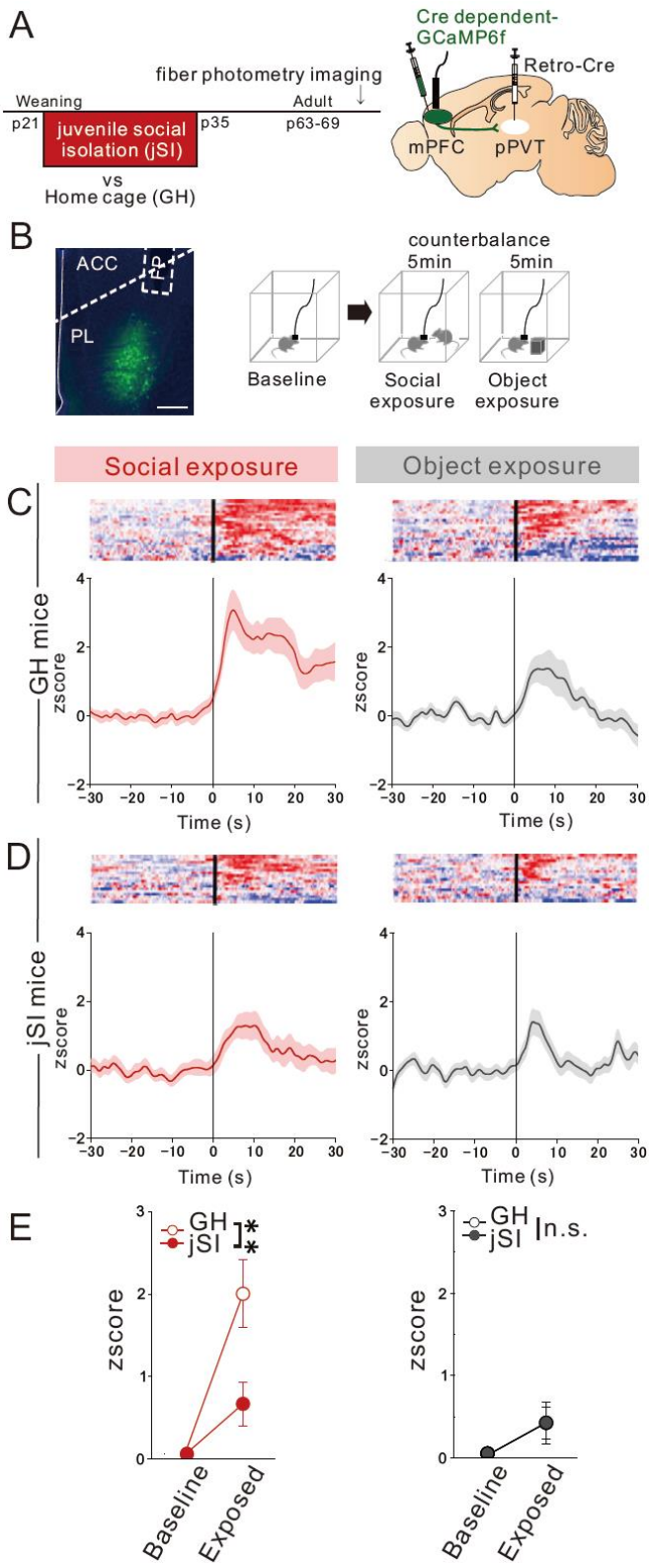

Fig1. Juvenile social isolation leads to failed activation of adult mPFC->pPVT projection neurons upon social exposure. (A) (Left) Timeline showing weaning at p21, and subsequent 2 weeks of juvenile social isolation (jSI), followed by re-housing or control group housing (GH), and subsequent In vivo fiber photometry calcium imaging of GCaMP6-expressing mPFC->pPVT neurons in behaving adult mice. (right) Selective viral expression of GCaMP6 in mPFC->pPVT projection neurons was achieved by injecting AAV8-DIO-GCaMP6f in mPFC and Retro AAV-cre in pPVT. **(B)** (Left) Representative localization of fiber ferrule and GCaMP6f expression in mPFC. Scale; 400um. (right) During fiber photometry imaging, mice were exposed to a novel mouse or novel object (order of object and social exploration was counterbalanced). **(C, D)** Heat maps of individual trials from one representative mouse (upper panel) and averaged traces of GCaMP6f signals from mPFC->pPVT neurons (lower panel) of **(C)** GH mice (23 mice) and **(D)** jSI mice (19 mice). **(E)** Social exposure evoked a lower response in jSI mice compared to GH mice, but object exposure evoked similar levels of activity in GH and jSI mice ($F_{3,80}$=7.798, ***P*=0.007; 2 way ANOVA), but no difference in response to a novel object ($F_{3,80}$=9.1262E-6, *P*=0.996; 2 way ANOVA).

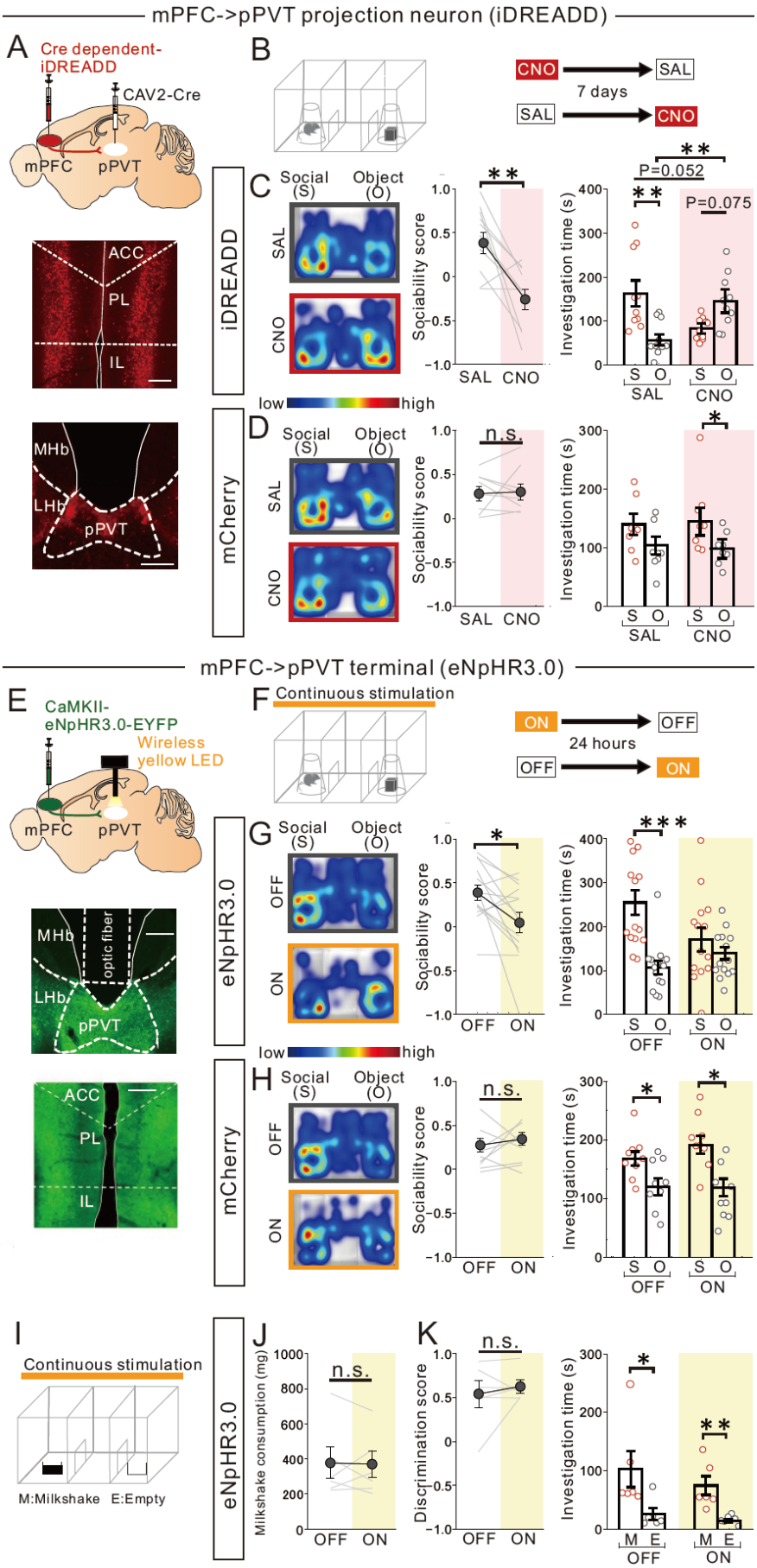

Fig2. mPFC-> pPVT projection neurons are necessary for sociability in adult group housed mice. **(A-D)** Chemogenetic suppression of mPFC->pPVT projection neurons. **(A)** (upper) cre-dependent Inhibitory DREADD (or mCherry) vector and a retrograde CAV2-Cre were injected into the mPFC and pPVT, respectively, to express iDREADD in mPFC->pPVT neurons. Representative images from mPFC (middle) and pPVT (lower) showing mCherry+iDREADD expression. **(B)** Group housed adult mice were treated with saline (SAL) or CNO (10mg/kg) and then underwent the 3 chamber test of social behavior. SAL and CNO session is counter-balanced for each behavior test with a 7-day interval between tests. **(C)** CNO-treated iDREADD+ mice showed reduced sociability, revealed by the reduced sociability scores (calculated as (Time; social-Time; object)/ (Time; social+ Time; object)) vs. SAL (t_9=3.548, ***P*=0.006, 10 mice; paired-t-test). Also, CNO treated iDREADD+ mice showed reduced social interaction ($\chi^2_{3,39}$=12.215, *P*=0.007, Kruskal-Wallis test; social vs CNO treated by SAL, ***P*=0.004: social vs object treated by CNO, *P*=0.075: SAL vs CNO exposed to social, *P*=0.052: 10mice; Mann-Whitney test). **(D)** However, control mCherry+ mice show no difference in sociability score (t_7=-0.191, *P*=0.854, 8 mice; paired-t-test) and investigation time ($\chi^2_{3,39}$=8.273, *P*=0.041, Kruskal-Wallis test; social vs object treated by CNO, *P*=0.015, 8mice; Mann-Whitney test). **(E-K)** Optogenetic suppression of mPFC->pPVT projection terminals. **(E)** (Upper) Halorhodopsin NpHR3.0 AAV under CamK2 promotor was injected into mPFC and mPFC->pPVT projection terminals were optically stimulated at the pPVT using a wireless yellow LED system. Representative images of mPFC (middle) and pPVT (lower) show selective transduction of halorhodopsin at injection areas in the mPFC and the projection target areas in pPVT where fiber ferrules are located. **(F)** Mice underwent the 3 chamber test of social behavior with (ON) or without (OFF) light stimulation. On and Off sessions were counter-balanced for each behavior test with a 24 hour interval between tests. **(G)** Mice with optogenetic suppression showed reduced sociability scores (t_{11}=2.769, **P*=0.016, 12 mice; paired-t-test) and reduced social interaction ($\chi^2_{3,55}$=18.165, *P*<0.001, Kruskal-Wallis test; social vs object treated by On, ****P*<0.001, 14mice; Mann-Whitney test). **(H)** However, control mCherry+ mice showed no difference in sociability score (t_8=-0.722, *P*=0.491, 9mice; paired-t-test) and investigation time ($\chi^2_{3,35}$=13.843, *P*=0.003, Kruskal-Wallis test; social vs object treated by On, **P*=0.024: social vs object treated by Off, **P*=0.040, 9mice; Mann-Whitney test). **(I)** Mice underwent for 3 chamber test of food preference with (ON) or without (OFF) light stimulation. On and Off session is counter-balanced for each behavior test with a 24 hour interval between tests. **(J)** Optogenetic suppression+ mice showed no difference in milkshake consumption (t_5=0.143, *P*=0.892, 6mice; paired-t-test). **(K)** Mice with optogenetic suppression showed no difference in discrimination score (t_5=-0.724, *P*=0.501, 6mice; paired-t-test) nor in investigation time ($\chi^2_{3,23}$=14.520, *P*=0.002, Kruskal-Wallis test; social vs object by off, **P*=0.026: social vs object treated by on, ***P*=0.002, 6mice; Mann-Whitney test). ***P<0.001, **P<0.01, *P<0.05.

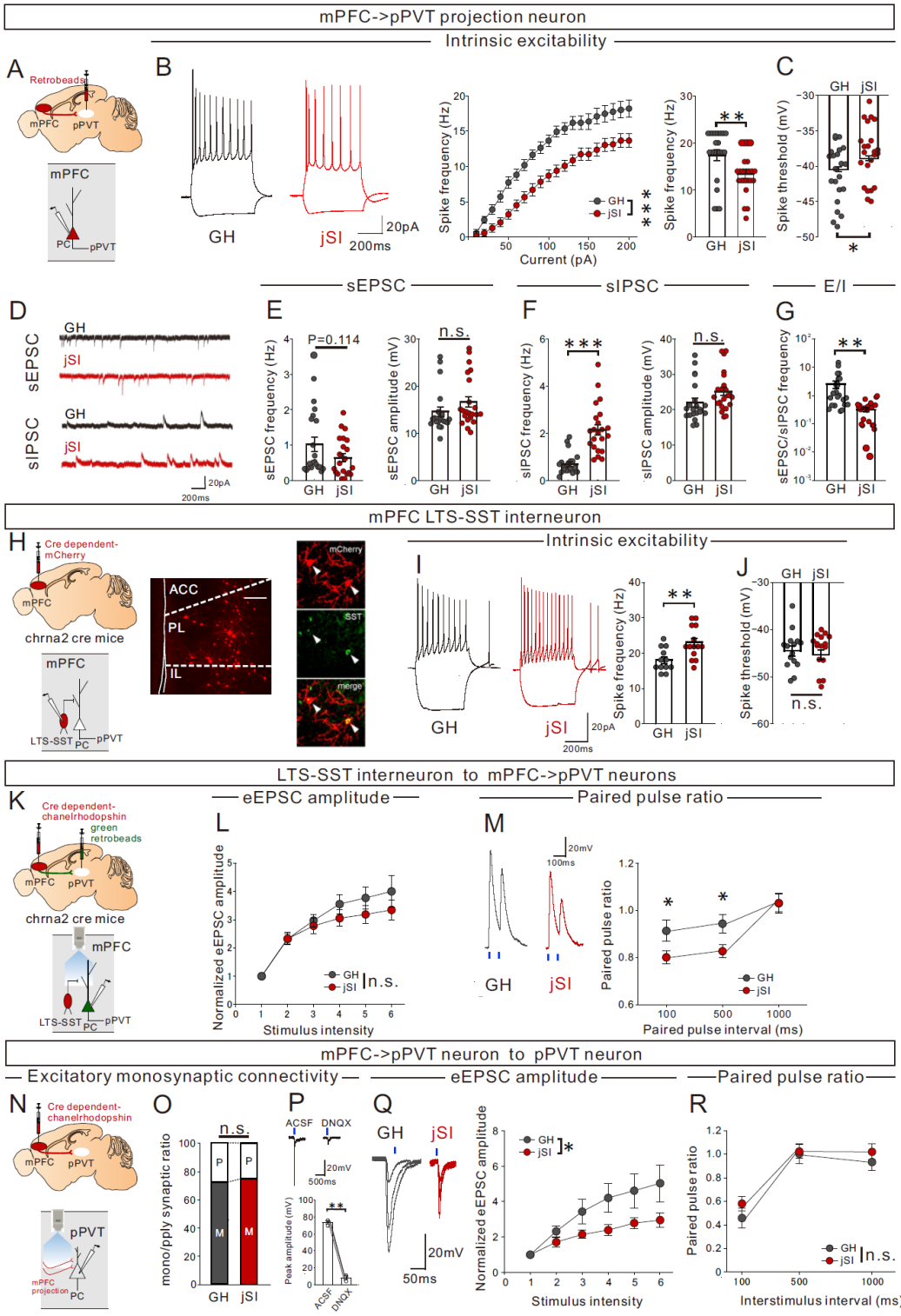

Fig3. jSI leads to reduced intrinsic excitability and increased inhibitory input drive of adult mPFC->PVT neurons. **(A-G)** Whole-cell patch clamp recording of adult mPFC->pPVT neurons from mPFC slices. **(A)** mPFC->pPVT neurons were labeled with retrobeads injected to pPVT after jSI (p21-p35) or GH (19-23 cells from 9 mice each). **(B)** (left) Assessment of intrinsic excitability of adult mPFC->pPVT neurons in the presence of DNQX (20μM), D-AP5 (50μM), and picrotoxin (30μM). Representative traces at 200pA injection recorded from mPFC ->pPVT neurons. (middle) Input-output curve showing a decreased spike frequency in adult jSI mice ($F_{1,14}$=21.185, ***P<0.001 jSI vs GH; ANOVA interaction). (right) Lower spike frequency at 200pA in jSI mice vs GH mice (t_{43}=2.919, **P=0.006; student t-test). **(C)** Higher spike threshold in jSI mice vs GH mice (t_{43}=-2.242, *P=0.03; student t-test). **(D)** Representative sPSCs. **(E)** sEPSC frequency in jSI mice was trending lower vs GH (t_{41}=1.616, P=0.114; student t-test) with no difference in sEPSC amplitude (t_{41}=-1.361, P=0.181; student t-test). **(F)** sIPSC frequency in jSI mice was significantly higher than in GH mice (t_{37}=-5.977, ***P<0.001; student t-test) and there was a not significant but trending increase in amplitude (t_{37}=-1.797, P=0.08; student t-test). **(G)** sEPSC/IPSC frequency ratio (E/I ratio) in jSI mice was significantly lower than in GH mice (t_{41}=2.918, **P=0.006; student t-test). **(H-J)** Whole-cell patch clamp recording from adult low threshold spiking (LTS)- somatostatin (SST) inter- neurons in mPFC slices after jSI or GH (10-14 cells from 7 mice each). **(H)** mPFC LTS-SST interneurons are fluorescently labeled by injecting cre-dependent mCherry vector to adult Chrna2-cre mice **(I)** (left) Assessment of intrinsic excitability of Chrna2+LTS-SST interneurons in the presence of DNQX (20μM), D-AP5 (50μM), and picrotoxin (30μM). Representative traces at 200pA injection recorded from mPFC->pPVT neurons. (right) Higher spike frequency at 200pA in jSI vs GH (t_{24}=-3.186 **P=0.004; student t-test). **(J)** There were no significant differences in spike threshold (t_{29}=0.574 P=0.570; student t-test). **(K-M)** Optogenetic interrogation of LTS-SST interneuron input onto mPFC->pPVT projection neurons. **(K)** Cre-dependent ChR2 vector and green retrobeads were injected into the mPFC and pPVT, respectively, to express ChR2 in LTS-SST interneurons and fluorescently label mPFC->pPVT neurons for patch-clamp recordings. **(L)** There were no significant differences in eEPSC amplitude ($F_{1,29}$=0.872, P=0.358 jSI vs GH; ANOVA interaction). **(M)** (left) eEPSCs are elicited by the optogenetic stimulation. Representative averaged waveform showing paired-pulse facilitation in eEPSCs at a 100-ms interval. Paired pulse ratio (PPR) is given by second evoked amplitude/first evoked amplitude. (right) PPR in jSI was significantly lower than in GH mice (100ms; t_{46}=2.130, *P=0.039, 500ms; t_{46}=2.392 *P=0.021, 1000ms; t_{46}=0.010 P=0.992; student paired t-test). **(N-R)** Optogenetic interrogation of mPFC->pPVT projection input onto pPVT neurons. **(N)** Channelrhodopshin encoding AAV2 was injected into the mPFC to express ChR2 in mPFC neurons. Whole cell patch-clamp recordings were performed while optogenetically activating mPFC->pPVT projection terminals in pPVT slices. **(O)** Excitatory connectivity was assessed by normalized postsynaptic currents (PSCs) recorded at -70 mV from pPVT neurons before and after application of tetrodotoxin (TTX; 1 μM) with 4-aminopyridine (4-AP; 100 μM). A majority of pPVT neurons received a monosynaptic input from mPFC. There was no difference in mono/polysynaptic ratio (t_{13}=-0.349, P=0.733; student t-test). **(P)** (upper) Optogenetic activation of mPFC->pPVT axons were blocked by DNQX (20 μM). pPVT neurons were clamped at–70 mV while optogenetocally stimulating mPFC-pPVT axons before and after bath application of DNQX. (bottom) Averaged amplitude decreases after application of DNQX (t_2=17.793, **P=0.003; paired t-test). **(Q)** (left) Representative eEPSC of pPVT neurons upon optogenetic activation of mPFC->pPVT axons in GH and jSI mice through gradually changing the intensity. (right) Line plots showing the relationship between stimulus intensity and normalized eEPSC amplitude. eEPSC amplitude was lower in jSI mice than GH mice ($F_{1,5}$=4.171, ***P=0.048 jSI vs GH; ANOVA interaction). **(R)** There were no significant differences in PPR (100ms; t_{29}=-1.189, P=0.244, 500ms; t_{29}=-0.200 P=0.843, 1000ms; t_{29}=-0.873 P=0.390; student t-test).